DOI: 10.1590/2317-488920160030285

ARTICLE

Chemostratigraphy of the lower Bambuí Group, southwestern São Francisco Craton, Brazil: insights on Gondwana paleoenvironments

Quimioestratigrafia da porção basal do Grupo Bambuí no sudoeste do Cráton do São Francisco: implicações para os paleoambientes de Gondwana

Matheus Kuchenbecker[1,2]*, Marly Babinski[3], Antônio Carlos Pedrosa-Soares[2], Leonardo Lopes-Silva[4], Felipe Pimenta[4]

ABSTRACT: The Bambuí Group, the most extensive carbonate-siliciclastic cover on the São Francisco craton, has been a matter of debate because of its potential correlations to global glacial events. Unfortunately, most available chemostratigraphic data came from samples collected on surface rock exposures, ever susceptible to the aggressive chemical weathering that characterizes the southeastern Brazil. On the other hand, we present here high-resolution chemostratigraphic studies based on C, O and Sr isotopic data from 53 samples collected along a weathering-free, continuous, 175 m thick sedimentary succession. This succession was recovered by borehole drilling in the southwestern São Francisco craton, where occur the Carrancas and Sete Lagoas formations, the lowermost units of the Bambuí Group. The drill cores reveal extremely irregular contacts between the basal diamictite and its basement, an Archaean foliated granodiorite. Geochronological and sedimentological data strongly suggest that the diamictite represents a lodgement till. This glaciogenic deposit is covered by a limestone succession which starts with impure carbonates showing aragonite pseudomorph fans and thin bands of black shale. The limestone pile grades to a marl-mudstone interval, which turns to a carbonate with biological components, succeeded by stromatolitic dolomite at the top. C and O isotopic signatures (referred to V-PDB) allow to the subdivision of the lower carbonate-pelite section into three intervals. The first isotopic interval corresponds to a cap carbonate, and displays negative values of $\delta^{13}C$ (*c.* -4‰), and a large oscillation of the $\delta^{18}O$ (-6 to -15‰). The Interval II shows a striking homoge-

RESUMO: *O Grupo Bambuí, mais importante unidade de cobertura do Cráton do São Francisco, tem sido alvo de intensos estudos e debates, entre outros motivos, pela possibilidade de correlação com eventos glaciais globais. A maior parte dos dados quimioestratigráficos disponíveis, no entanto, provém de amostras coletadas em afloramentos, sujeitos a expressivo intemperismo químico. Neste trabalho, é apresentado um levantamento quimioestratigráfico de alta resolução, baseado em análises de C, O e Sr realizadas em 53 amostras coletadas em 175 m de sequência sedimentar contínua, livre de intemperismo. Tal sequência foi obtida a partir de testemunhos de sondagem realizada na porção sul do Cráton do São Francisco, onde ocorrem rochas das formações Carrancas e Sete Lagoas, as mais basais do Grupo Bambuí. Os testemunhos revelaram contato extremamente irregular entre uma camada de diamictito e seu embasamento, um granodiorito foliado de idade arqueana. Dados sedimentológicos e geocronológicos indicam que o diamictito representa um tilito de alojamento, que apresenta contato brusco com a sequência carbonática sobrejacente. Essa sequência se inicia com calcário impuro, que exibe leques de cristais pseudomorfos de aragonita e delgadas camadas de folhelho negro. O calcário passa gradacionalmente para um intervalo argiloso, que por sua vez volta a gradar para uma espessa sequência de calcário com laminação microbiana, sucedido por dolomito estromatolítico no topo da coluna. As assinaturas isotópicas de C e O permitem a identificação de três intervalos distintos. O Intervalo I, basal, corresponde a um carbonato de capa, exibindo valores negativos de $\delta^{13}C$ (*c.* -4‰), e grande oscilação nos valores de $\delta^{18}O$ (-6 a -15‰). O Intervalo II exibe marcante homogeneidade nos valores de $\delta^{13}C$ e $\delta^{18}O$, que se situam em torno de 1‰ e -7‰, respecti-*

[1]Laboratório de Estudos Tectônicos/Núcleo de Geociências e Instituto de Ciência e Tecnologia, Universidade Federal dos Vales do Jequitinhonha e Mucuri, Diamantina (MG), Brazil.

[2]Centro de Pesquisa Professor Manoel Teixeira da Costa, Instituto de Geociências, Universidade Federal de Minas Gerais – UFMG, Belo Horizonte (MG), Brazil. *E-mail: mk.geologia@gmail.com, pedrosa@pq.cnpq.br*

[3]Centro de Pesquisas Geocronológicas, Instituto de Geociências, Universidade de São Paulo – USP, São Paulo (SP), Brazil. *E-mail: babinski@usp.br*

[4]Lhoist do Brasil, São José da Lapa (MG), Brazil. *E-mail: leogeo83@gmail.com, felipegeologia@gmail.com*

*Corresponding author.

Manuscript ID: 30285: **Received in:** 04/21/2015. **Approved in:** 02/12/2016.

neity in $\delta^{13}C$ and $\delta^{18}O$, around 1‰ and -7‰, respectively. At the top, Interval III shows a large positive excursion of the $\delta^{13}C$ (up to 8‰) and $\delta^{18}O$ (-8 to -3‰) values. Unaltered $^{86}Sr/^{87}Sr$ ratios range from 0.7075 to 0.7077, mainly at the top of the section. The geochemistry of the carbonates is controlled by their terrigenous content (mostly quartz and clay minerals) which is concentrated in the lower units. Samples free of terrigenous contamination show Y/Ho ratios ranging from 25 to 50, suggesting a freshwater input during carbonate deposition. It is concluded that the diamictite has a glaciogenic origin and is covered by a cap carbonate. This pair has been identified along the basin and is related to one of the main Neoproterozoic glaciations. Discrepancy between the $^{86}Sr/^{87}Sr$ values and the global variation curves can be related to freshwater input during the carbonate deposition. Based on the regional tectonic context, the Bambuí Basin may have been a restricted marine basin, totally or partially surrounded by mountain ranges within Gondwana, in the Neoproterozoic/Paleozoic boundary. In its early stages, the sedimentation was influenced by a global glacial event, whose melting phase was responsible by freshwater input in the basin. The gradual rise of the temperature was followed by an increase of the biological activity. Finally, a sudden increase in the biological activity could have been driven by paleogeographic changes caused by the active tectonic.

KEYWORDS: Bambuí Group; Chemostratigraphy; São Francisco Craton; Neoproterozoic; Gondwana

vamente. No topo, o Intervalo III exibe uma grande excursão positiva dos valores de $\delta^{13}C$ (até 8‰) e $\delta^{18}O$ (-8 a -3‰). Razões $^{87}Sr/^{86}Sr$ variam entre 0,7075 e 0,7077, obtidas exclusivamente em amostras do topo da sequência. A assinatura geoquímica das rochas carbonáticas mostrou-se fortemente controlada pelo conteúdo terrrígeno, concentrado sobretudo nas unidades mais basais. Amostras livres da influência de elementos terrígenos mostram razões Y/Ho variando entre 25 e 50, o que sugere a influência de água doce durante a deposição dos calcários. Com base nos dados obtidos, conclui-se que a porção basal da sequência estudada representa um par "diamictito-carbonato de capa" relacionado a um dos eventos glaciais que ocorreram entre o fim do Neoproterozoico e o início do Paleozoico. Além disso, discrepâncias nas razões $^{87}Sr/^{86}Sr$, quando comparadas às curvas globais de evolução isotópica, podem ser atribuídas à influência da água doce em um ambiente marinho restrito. Tendo-se em vista o contexto regional, a Bacia Bambuí representaria, no limite Neoproterozoico/Paleozoico, uma bacia marinha restrita, total ou parcialmente circundada por cadeias de montanhas, no interior de Gondwana. Em seus estágios iniciais, a sedimentação teria ocorrido sob influência de um episódio glacial, cuja fase de degelo foi responsável por significativa entrada de água doce no mar. Com o gradual aumento de temperatura, a atividade biológica no mar teria aumentado progressivamente. Por fim, um súbito aumento na atividade biológica pode ter sido catalisado por mudanças paleogeográficas causadas pela tectônica ativa.

PALAVRAS-CHAVE: *Grupo Bambuí; Quimioestratigrafia; Cráton do São Francisco; Neoproterozoico; Gondwana*

INTRODUCTION

Since the 1990's, the Neoproterozoic climatic changes have been of worldwide interest. In the study of these phenomena, special attention is given to the couple diamictite-carbonate that records in some places abrupt icehouse-greenhouse fluctuations (e.g. Hoffman *et al.* 1998, Hoffman & Schrag 2002, Gómez-Peral *et al.* 2007). The paucity of fossils in most Neoproterozoic deposits, however, complicates the establishment of temporal and areal correlations between the several occurrences of these pairs worldwide (Melezhik *et al.* 2001, Jacobsen & Kaufman 1999).

Light stable isotope geochemistry, including carbon and oxygen, is the most widely applied chemostratigraphic tool to investigate the Neoproterozoic rock record, yielding important results in paleoenvironmental and tectonic analysis, and assisting in the establishment of regional or global correlations (Jacobsen & Kaufman 1999, Mehlezik *et al.* 2001, Halverson *et al.* 2005, Delpomdor & Preat 2013). After more than three decades of chemostratigraphic studies, the secular $^{87}Sr/^{86}Sr$ and $\delta^{13}C$ trends in Phanerozoic seawater are now well-established, and our understanding of Precambrian seawater isotopic patterns and its significance has substantially increased. Large negative $\delta^{13}C$ excursions are remarkable features of the Neoproterozoic Era (Knoll *et al.* 1986, Kaufman *et al.* 1991, Shields & Veizer 2002, Halverson *et al.* 2010) that have been considered as a consequence of multiple glaciations marked by rapid precipitation of overlying cap carbonates (Hoffman *et al.* 1998, Figueiredo 2010). Globally, at least three major glacial events exhibit these features: Sturtian (c. 720 Ma), Marinoan (c. 635 Ma) and Gaskiers (c. 580 Ma). On the other hand, positive $\delta^{13}C$ excursions are most explained by an increase in the fraction of organic carbon fraction during burial (Knoll *et al.* 1986), sometimes associated with tectonic events (Santos *et al.* 2000).

In east-central Brazil, the Bambuí Basin covers most of the São Francisco Craton, showing some glacial deposits in the Carrancas Formation, which is covered by a thick carbonate unit known as Sete Lagoas Formation. The tectonic setting of the basin is complex, considering that its evolution is linked to the development of two orogenic belts and, during their final stages, it was completely surrounded by mountain belts, in a complicated scenario that would possible favor a restricted basin, with no connection with the global ocean. This singular scenario provides a special target to apply chemostratigraphy in order to examine the paleoenviroment and its possible relation with tectonics.

The Arcos region, located in the southwestern portion of the basin (Fig. 1), is known in the geological literature by the extensive occurrence of carbonate rocks of the Sete Lagoas Formation, Bambuí Group. In this region, many limestone quarries are mined to produce cement and lime.

In this paper, we present new isotopic data obtained from rock samples collected from two drillcores obtained by a mining company of the region. The boreholes provided

access to a 175 m thick section totally free of weathering, a rare situation in a country marked by tropical weather.

GEOLOGIC SETTING

The basement of the southern São Francisco Craton consists of an Archean block surrounded to the south by a late Rhyacian orogenic belt (Noce *et al.* 2000, 2007). In Arcos region, the basement comprises orthogneisses, amphibolites and meta-ultramafic rocks, with minor schists and quartzites, intruded by gabbronorites, granitoids and gabbros (Fernandes & Carneiro 2000, Oliveira & Carneiro 2001).

The Neoproterozoic sedimentary rocks of the Bambuí Basin overlie these complexes lie, and covers a large part of the craton. This basin includes a basal diamictite-bearing unit, Carrancas Formation, covered by the pelite-carbonate succession of the Bambuí Group. The regional geotectonic setting (Fig. 1) indicates that the basin represents a complex foreland system resulting from the interaction of crustal loads promoted by both the Brasília belt and the Araçuaí Orogen in the São Francisco paleoplate (Kuchenbecker 2014, Martins-Neto *et al.* 2001, Martins-Neto 2009, Coelho *et al.* 2008).

The Carrancas Formation crops out discontinuously at the southern portion of the basin, and was recognized in some other places through borehole information (e.g. Kuchenbecker *et al.* 2013, Reis & Suss, 2014). The unit comprises mainly diamictite, siltstone and rhythmite, which at some places are directly covered by the carbonate rocks of the Sete Lagoas Formation. Glacial features in the Carrancas Formation include boulder dropstones in rhytmite (Romano & Knauer 2003) and thin layers of lodgment tillite showing subglacial shear and clast orientation (Kuchenbecker *et al.* 2013).

In the southeastern portion of the basin, the basal portion of the Sete Lagoas Formation is considered as a post-glacial "cap carbonate", based on the sedimentary facies and C-O isotopic pattern (Vieira *et al.* 2007). Babinski *et al.* (2007) obtained a Pb-Pb isochron age of 740 ± 22 Ma for this cap carbonate and correlated it to the Sturtian glaciation. However, zircon populations of about 610 Ma (Rodrigues 2008, Pimentel *et al.* 2011) and 550 Ma (Paula-Santos *et al.* 2015, Pimentel *et al.* 2012) were found in shales interbedded into the Sete Lagoas Formation limestones, indicating an Ediacaran age for the Bambuí Group. This age was also corroborated by the presence of the late Ediacaran index fossil *Cloudina* (Gaucher & Germs 2009 and references therein), recently described in the same rocks by Warren *et al.* (2014).

Stratigraphy and petrography

The two studied drillcores were described in detail, allowing the identification of the Carrancas and Sete Lagoas formations, besides the crystalline basement. Based on the facies distribution, ten informal units were described by Kuchenbecker *et al.* (2011, 2013, Fig. 2).

The basement is represented by a fine- to medium-grained, dark green to gray granodiorite, which shows a discrete foliation. This rock is composed by quartz, plagioclase, microcline

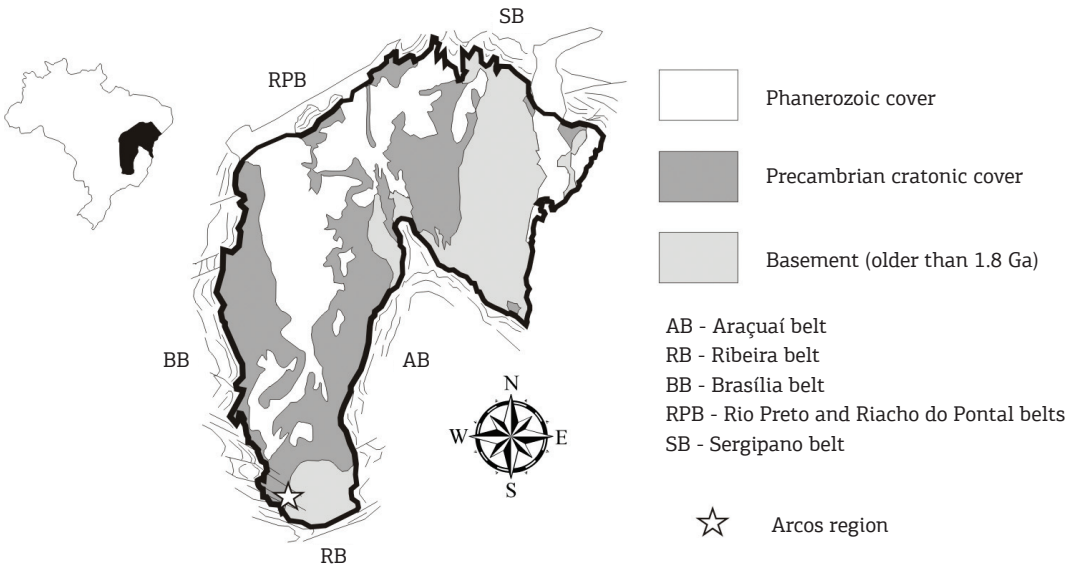

AB: Araçuaí Belt; RB: Ribeira Belt; BB: Brasília Belt; RPB: Rio Preto and Riacho do Pontal belts; SB: Sergipana Belt.

Figure 1. Location of Arcos region in the São Francisco Craton.

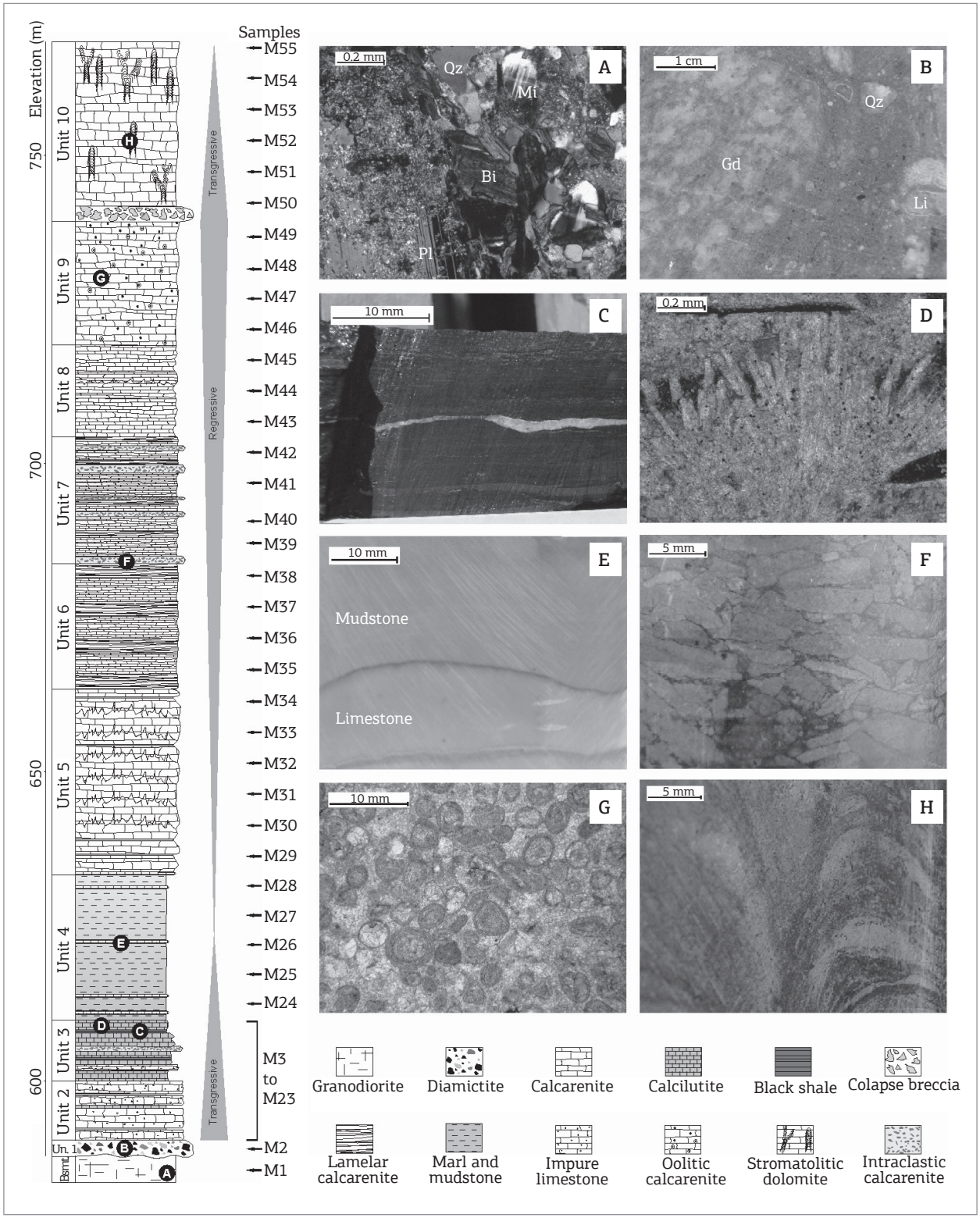

Figure 2. Stratigraphic section of the basal Bambuí Group at Arcos, southwestern São Francisco Basin, Brazil. (A) Photomicrography of the basal granodiorite (Polarized light); Pl: plagioclase, Bi: biotite, Mi: microcline, Qz: quartz; (B) Carrancas Formation (Unit 1) diamictite. Clasts of granodiorite – Gd, quartz – Qz and limestone – Li; (C) Unit 3 black shale; (D) Aragonite pseudomorph fans (Polarized light); (E) Centimetric limestone layer in the Unit 4 mudstone; (F) Intraclastic layer, Unit 7; (G) Photomicrography of Unit 9 oolitic limestone; (H) Columnar stromatolites of Unit 10.

and biotite as essential minerals, and monazite, sphene, zircon and garnet as accessory minerals. Epidote and carbonate record incipient hydrothermal alteration. U-Pb analysis on zircons reveals an Archean age of c. 2.9 Ga for this rock (Kuchenbecker *et al.* 2013).

The lowermost sedimentary unit is the Carrancas Formation (Unit 1), a ~0,5 m thick diamictite, with sub-rounded to angular granule- to cobble-sized clasts of granodiorite, carbonate, siltstone, quartz and calcite, supported by a greenish matrix of fine sand and mud. The contact with the basement is highly irregular and the clasts show a preferential orientation. Based on its sedimentary features, Kuchenbecker *et al.* (2013) interpreted the diamictite as a lodgment tillite. In the same paper, the authors report that U-Pb ages from detrital zircon grains recovered from the diamictite yield a narrow Archean range around 2.9 Ga, indicating a local source for the sediments.

The tillite is covered by the Sete Lagoas Formation, whose basal unit (Unit 2) is a 9 m thick layer of light gray, impure calcarenite, with sub-rounded to angular, granule- to sand-size clasts of quartz, mica, granite and chloritite. Centimetric beds of gray mudstone often occur.

Unit 3 is an 8 m thick carbonate succession of gray calcilutite to fine calcarenite, with some layers of carbonatic shale. Cross lamination occurs at the bottom of the unit and, at the top, millimetric-size aragonite pseudomorph fans are clearly observed. The carbonate content of Unit 3 decreases toward the top, where intercalations of green marl become abundant and record a gradational contact with Unit 4.

A 12 m thick succession of green marl and mudstone characterizes the Unit 4. Both contacts, bottom and top, of this unit are gradational and marked, at the bottom and top, by the occurrence of centimetric layers of white to pink carbonate.

Unit 5 is a 30 m thick succession of massive, light gray calcarenite, with widespread stylolites. Unit 6 consists of a 31 m thick pile of gray calcarenite, with alternating lamellar intercalations and remarkable occurrence of microbial lamination. The 17 m thick Unit 7 is similar to Unit 6, but shows some centimetric to decimetric intraclastic horizons with elongated and sub-rounded micritic clasts, generally oriented with the bedding.

Unit 8 is defined by a sharp decrease of lamellar horizons, giving place to a 14 m thick interval with frequent granulometric variations from calcarenite to calcisiltite. A 21 m thick homogeneous pile of massive, fine to medium-grained, locally intraclastic, oolitic to pisolitic calcarenite characterizes Unit 9.

Unit 10 occurs at the top of the drill cores, and is composed by a basal metric layer of collapse breccia, followed by a thick succession of dolomite with columnar stromatolites.

The lithofacies succession suggests a transgressive-regressive cycle with the onset of a new transgressive event at the top. The lower sedimentary units also suggest significant change of source areas during the beginning of the basin filling. The aragonite fans are similar to those found in the Sete Lagoas Formation in other parts of the basin (e.g. Vieira *et al.* 2007, Alvarenga *et al.* 2012).

METHODS

The use of drillcores offers the rare opportunity of sampling a complete section without the effect of subaerial exposure, greatly favoring the geochemical and petrographic studies. Fifty-five samples were collected along the whole section, in intervals of 5 m or shorter considering the rock heterogeneities. Each carbonate sample was studied in detail in thin section, and the non-altered portions of the carbonate slices were sampled using microdrilling.

Analyses of Sr, C and O isotopes were carried out at the Center of Geochronological Research (CPGeo), at the University of São Paulo. Carbonate samples for Sr analysis were first leached with HCl 0.1M and the supernatant was discarded. Analysis was conducted on the second leachate obtained with HCl 1.0 M. Solutions were converted to HNO_3 2M and loaded through Sr-SPEC resin, and the Sr was eluted with HNO_3 0.05M. The Sr was loaded onto a Ta filament and analyzed with a Finnigan MAT 262 thermal ionization mass spectrometer. The data were corrected for mass fractionation using $^{86}Sr/^{88}Sr = 0.1194$.

For C and O isotope analyses, CO_2 gas was extracted from powdered carbonates in a high vacuum line after reaction with 100% phosphoric acid at room temperature for 24 h. Following cryogenic cleaning, the released CO_2 was analyzed in a DELTA Advantage mass spectrometer, using IAEA standards, as well as a secondary standard. Results are reported in conventional notation in per mil (‰) relative to the V-PDB (Vienna-Pee Dee Belemnites) standard. The uncertainties of isotope measurements are 0.1‰ for both carbon and oxygen.

Analysis of major, trace and REE elements were carried out in the ACME (Canada) and GEOSOL (Brazil) facilities. Total abundances of the major oxides and several minor elements were reported on a 0.2 g sample analyzed by ICP-emission spectrometry following a Lithium metaborate/tetraborate fusion and dilute nitric digestion. Loss on ignition (LOI) was determined by weigh difference after ignition at 1,000°C. Rare earth and refractory elements were determined by ICP mass spectrometry following a Lithium metaborate/tetraborate fusion and nitric acid digestion of a 0.2 g sample. In addition, a separate 0.5 g split was digested

in Aqua Regia and analyzed by ICP mass spectrometry to report the precious and base metals.

RESULTS

Lithogeochemistry

The lithogeochemical results are displayed in Table 1, with the chemical classification of the carbonate rocks based on their Mg/Ca ratios (values after Figueiredo 2006). According to this classification, dolostones occur in Units 3 and 10, and magnesium limestone contribution occurs in units 4, 6 and 7.

The Units 2 and 3 show very heterogeneous composition, higher terrigenous content and black shale intercalations. The high concentrations of Na, Mn and P in some samples could indicate the presence of minerals such as phosphates or the adsorption of these elements on the clay minerals.

Unit 4 shows high concentrations of lithophile elements, reflecting its pelitic-marly composition. A particularity is the low Na/K ratio, which can be directly related to the clay mineralogy.

Table 1. Major elements data from Sete Lagoas Formation at Arcos, Minas Gerais. Values in percentage.

Sample	SiO_2	Al_2O_3	Fe_2O_3	CaO	MgO	TiO_2	P_2O_5	Na_2O	K_2O	MnO	LOI	Mn/Sr	TOT/C	TOT/S
M3	12.19	2.80	2.74	25.45	17.69	0.16	0.04	0.24	0.25	0.07	38.00	**5.89**	10.42	0.87
M5	9.20	2.14	1.57	29.60	17.20	0.15	0.08	0.29	0.10	0.04	40.03	_	_	_
M7	21.20	5.65	3.58	24.20	11.70	0.32	0.13	0.71	1.34	0.06	28.24	_	_	_
M9	27.00	6.86	3.57	29.10	5.61	0.36	0.70	1.01	0.70	0.06	24.75	_	_	_
M11	17.90	2.61	3.33	26.60	13.40	0.14	0.09	<0.1	0.57	0.38	35.18	_	_	_
M13	18.20	2.53	1.83	26.30	14.10	0.10	0.03	0.13	0.76	0.13	35.56	_	_	_
M15	16.80	2.06	1.62	27.40	14.10	0.10	0.04	0.12	0.61	0.15	36.48	_	_	_
M16	30.46	7.01	3.40	19.37	10.03	0.34	3.92	0.28	2.03	0.09	22.70	**2.67**	6.15	1.80
M17	18.75	3.68	1.31	25.92	12.75	0.16	1.12	0.18	1.17	0.13	34.50	**4.91**	9.27	0.20
M19	8.24	1.93	0.81	31.70	15.60	0.11	0.04	<0.1	0.69	0.15	40.69	_	_	_
M21	23.40	4.57	2.19	22.80	12.60	0.23	0.06	0.27	1.47	0.40	31.19	_	_	_
M25	55.04	10.97	5.09	7.06	5.95	0.51	0.11	0.34	3.28	0.05	11.40	3.10	2.51	<0.02
M27	9.10	1.87	1.18	47.40	1.38	0.13	0.04	0.19	0.54	0.03	37.14	_	_	_
M29	0.80	0.17	0.11	54.80	0.85	0.04	0.01	<0.1	0.07	<0.01	43.33	_	_	_
M31	1.72	0.60	0.20	52.30	1.14	0.04	0.03	<0.1	0.19	<0.01	42.68	_	_	_
M33	0.44	0.06	<0.04	55.18	0.47	<0.01	0.02	<0.01	0.03	<0.01	43.70	0.22	12.31	0.02
M35	0.92	0.38	0.12	51.50	3.22	0.04	0.08	<0.1	0.10	<0.01	43.51	_	_	_
M37	0.41	0.06	<0.04	54.91	0.94	<0.01	0.04	<0.01	0.03	<0.01	43.50	0.14	12.19	<0.02
M39	2.63	0.33	0.10	53.60	0.37	0.04	0.11	<0.1	0.05	<0.01	42.39	_	_	_
M41	0.66	0.14	0.05	44.75	9.03	<0.01	0.22	<0.01	0.06	<0.01	44.90	0.16	12.39	0.02
M43	0.22	<0.1	0.04	55.30	0.24	0.02	0.05	<0.1	0.01	<0.01	43.64	_	_	_
M45	0.73	0.02	<0.04	55.57	0.21	<0.01	0.07	<0.01	0.02	<0.01	43.10	0.04	12.03	<0.02
M46	0.30	0.18	0.01	54.90	0.20	0.02	0.05	<0.1	<0.01	<0.01	43.52	_	_	_
M48	0.21	<0.01	<0.04	55.89	0.14	<0.01	0.07	<0.01	0.01	<0.01	43.20	0.02	12.09	<0.02
M50	1.94	0.19	0.15	31.73	18.79	<0.01	<0.01	0.02	0.07	0.01	46.70	0.35	12.63	0.04
M52	0.92	0.15	0.10	33.60	18.60	0.02	<0.01	<0.1	0.08	<0.01	46.21	_	_	_

Rb/Sr ratios reflect the relative abundance of terrigenous content and the carbonate fraction. As expected, Units 2 and 3 show the highest Rb/Sr values (up to 3.6), while in the more carbonate units the ratio is usually low (down to 0.0008). It is observed, however, that slightly higher Rb/Sr ratios are associated with the dolomitized portions, reflecting the low affinity of dolomite with Sr, which is preferentially retained by calcite due to the similarity of its ionic radius with Ca. Due to this, Sr loss during diagenesis is a common feature associated with the dolomite genesis (e.g. James & Jones 2015, Bartley *et al.* 2007).

In general, the whole section shows very low concentrations in all trace elements, except for Units 2, 3 and 4, which shows enrichment in Zn, Co and Cu relative to the standard limestone, probably due to its high terrigenous content.

The REE+Y concentrations (Table 2) were normalized to the *Post-Archean Australian Shale* (PAAS by McLennan, 1989; Fig. 3)

Units 5 to 10 show low REE fractionation, with lower concentrations than the PAAS and a slightly depletion of the LREE. Discrete Y-positive and Pr-negative anomalies are observed, indicating a typically marine genesis (Frimmel 2008).

According to McLennan (1989), the REE content in sedimentary rocks can be controlled, among other factors, by the terrigenous phases within the rock. In the case of carbonate rocks, the presence of detrital terrigenous minerals should cause significant alterations in the patterns (Frimmel 2009). Thus, Zr concentrations were used to monitor the presence of detritic phases which can change the primary REE pattern. As proposed by Frimmel (2009), a Zr concentration of 4 ppm was taken as the limit to identify samples free of contamination. It is important to highlight that, according to some authors, the REE patterns are usually not affected by diagenesis (*e.g.* Zhao *et al.* 2009) or dolomitization (McLennan 1989).

The total REE of the pure limestones (2.5 to 8.2 ppm) is much lower than the standard PAAS (184.4 ppm) and NASC (173 ppm), and is also lower than other Late Neoproterozoic

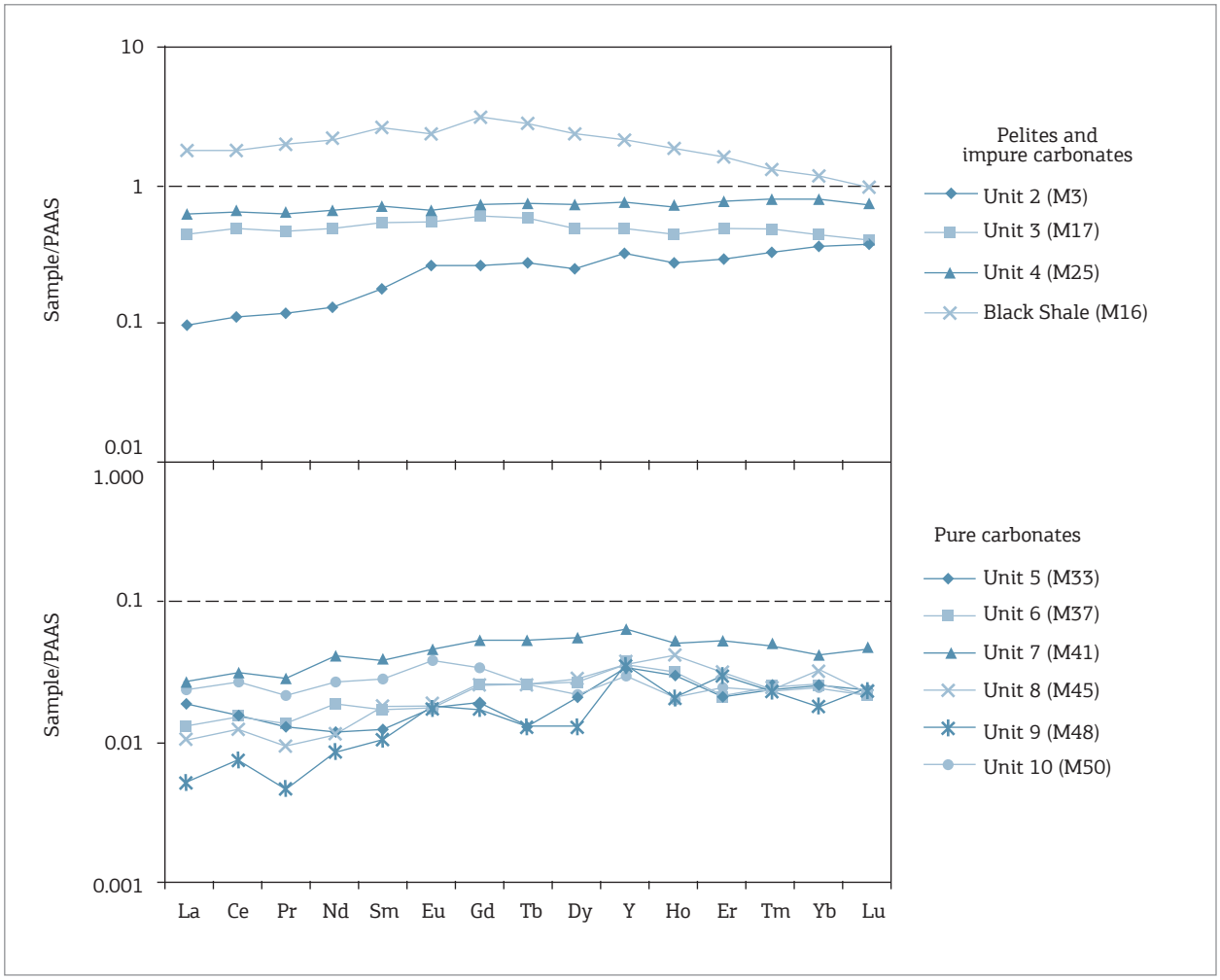

Figure 3. REE+Y patterns for the studied pelites, impure carbonates (up) and pure carbonates (down).

Table 2. Trace element and REE data from Sete Lagoas Formation at Arcos, Minas Gerais. Values in ppm.

	M16	M3	M17	M25	M33	M37	M41	M45	M48	M50
Au	<0.5	<0.5	<0.5	<0.5	<0.5	<0.5	<0.5	<0.5	<0.5	<0.5
Ba	355.00	44.00	227.00	451.00	9.00	11.00	20.00	18.00	37.00	24.00
Be	1.00	<1	1.00	3.00	<1	<1	<1	<1	<1	<1
Co	29.70	26.60	8.60	23.30	6.60	4.00	4.60	5.80	2.30	8.00
Cs	6.70	2.90	3.10	10.00	<0.1	0.10	0.30	<0.1	<0.1	0.30
Ga	9.20	3.40	5.10	15.30	<0.5	<0.5	<0.5	<0.5	<0.5	<0.5
Hf	1.70	0.70	0.90	2.80	0.10	<0.1	0.10	<0.1	<0.1	<0.1
Nb	6.10	1.80	2.90	10.50	<0.1	0.10	0.20	<0.1	<0.1	0.20
Ni	54.00	123.00	<20	46.00	<20	<20	<20	<20	<20	<20
Rb	95.30	12.80	56.20	139.20	1.20	1.20	2.40	0.60	0.30	3.50
Sc	9.00	6.00	4.00	11.00	<1	<1	<1	<1	<1	<1
Sn	1.00	<1	<1	2.00	<1	<1	<1	<1	<1	<1
Sr	261.20	92.10	205.20	124.90	321.30	513.70	426.80	1890.20	3620.80	220.50
Ta	0.50	0.30	0.20	0.80	<0.1	<0.1	<0.1	<0.1	<0.1	<0.1
Th	31.90	5.30	8.50	11.40	<0.2	<0.2	<0.2	<0.2	<0.2	0.20
U	13.20	1.80	3.70	4.10	0.50	1.20	2.50	0.70	1.50	0.60
V	83.00	26.00	36.00	66.00	<8	<8	<8	<8	<8	<8
W	107.60	71.40	51.00	85.10	51.60	35.30	36.20	47.80	24.90	53.20
Zr	66.60	28.40	34.00	107.10	2.60	1.90	3.50	0.80	0.80	2.30
Ag	<0.1	<0.1	<0.1	<0.1	<0.1	<0.1	<0.1	<0.1	<0.1	<0.1
As	15.60	6.90	2.40	<0.5	4.00	4.30	4.60	5.00	5.10	3.90
Bi	0.20	<0.1	<0.1	<0.1	<0.1	<0.1	<0.1	<0.1	<0.1	<0.1
Cd	0.50	0.50	<0.1	<0.1	<0.1	<0.1	<0.1	<0.1	<0.1	<0.1
Cu	20.80	13.60	6.20	0.80	3.50	0.20	2.90	1.30	7.10	5.20
Hg	0.10	<0.01	<0.01	<0.01	<0.01	<0.01	<0.01	0.02	<0.01	<0.01
Mo	2.30	0.20	<0.1	0.10	<0.1	<0.1	0.20	<0.1	0.10	0.10
Ni	50.70	113.20	8.40	26.90	5.00	4.00	4.10	5.20	3.30	4.80
Pb	11.60	7.80	0.90	1.20	0.40	0.60	0.50	0.50	7.00	2.10
Sb	0.50	0.30	<0.1	<0.1	<0.1	<0.1	<0.1	<0.1	<0.1	<0.1
Se	1.30	<0.5	<0.5	<0.5	<0.5	<0.5	<0.5	<0.5	<0.5	<0.5
Tl	0.20	<0.1	<0.1	<0.1	<0.1	<0.1	<0.1	<0.1	<0.1	<0.1
Zn	117.00	30.00	20.00	56.00	2.00	<1	2.00	15.00	4.00	7.00
La	3.60	68.90	16.70	23.10	0.70	0.50	1.00	0.40	0.20	0.90
Ce	8.50	143.60	36.30	50.10	1.20	1.20	2.60	1.00	0.60	2.10
Pr	1.01	17.15	4.01	5.57	0.12	0.12	0.24	0.08	0.04	0.19
Nd	4.40	72.50	15.50	21.90	0.40	0.60	1.40	0.40	0.29	0.90

Continue...

Table 2. Continuation.

	M16	M3	M17	M25	M33	M37	M41	M45	M48	M50
Sm	0.97	14.42	2.96	3.86	0.07	0.09	0.22	0.10	0.06	0.15
Eu	0.28	2.41	0.59	0.73	0.02	0.02	0.05	0.02	0.02	0.04
Gd	1.19	14.23	2.71	3.43	0.09	0.11	0.24	0.11	0.08	0.15
Tb	0.21	2.10	0.42	0.57	0.01	0.02	0.04	0.02	0.01	0.02
Dy	1.17	11.06	2.31	3.31	0.10	0.12	0.26	0.13	0.06	0.10
Y	8.30	56.70	13.40	20.00	0.90	1.00	1.80	1.00	1.00	0.80
Ho	0.27	1.78	0.43	0.68	0.03	0.03	0.05	0.04	0.02	0.02
Er	0.80	4.42	1.31	2.13	0.06	0.06	0.15	0.09	0.08	0.07
Tm	0.13	0.53	0.19	0.32	0.01	0.01	0.02	0.01	0.01	0.01
Yb	1.00	3.14	1.17	2.15	0.07	0.07	0.12	0.09	0.05	0.07
Lu	0.16	0.41	0.17	0.32	0.01	0.01	0.02	0.01	0.01	0.01

limestones worldwide (e.g. limestones from the northern Anhui Province, China – 9.6 to 54.2 ppm, Song *et al.* 2014).

One of the best parameters to investigate carbonate genesis is the Y/Ho ratio. Despite having a very similar behavior due to their identical ionic radius and charge, Ho is removed from seawater two times faster than Y. Thus, the typical seawater Y/Ho ratio is between 60 and 90, while the values for river water are closer to crustal values (c. 26 – 27), but below the seawater average (Frimmel 2009). The non altered samples show Y/Ho ratio between 25 and 50, with 35.7 as average value.

Carbon and Oxygen isotopes

The C and O isotopic data are displayed in Table 3. In the Units 2, 3 and 4, marked by the presence of terrigenous phases, the analyses were performed in pure, centimetric carbonate layers.

The isotopic section (Fig. 4) shows three distinct chemostratigraphic intervals, from base to top. The Interval I is characterized by negative $\delta^{13}C$ values (-5 to -3‰) at the bottom (Unit 2) and more positive values to the top, close to 0‰ (Unit 3). At the top of Unit 3, the $\delta^{13}C$ values turn to negative (c. -1.5‰), and then close to 0‰ again. In these intervals, $\delta^{18}O$ values are very heterogeneous, oscillating between -6 and -15‰.

The Interval II is isotopically more constant and corresponds to the Units 4 to 9. The $\delta^{13}C_{PDB}$ values are around 1‰ in the whole interval, with only a little excursion to 0‰ at 700 m. The $\delta^{18}O_{PDB}$ values range between -6 and -8.5 ‰, with a sharp positive excursion following the $\delta^{13}C$ pattern.

Interval III corresponds to the Unit 10, starting immediately after the collapse breccias. It is characterized by a strong positive excursion of the $\delta^{13}C_{PDB}$ values, which jump from near 2 to above 7.5‰. In this interval, $\delta^{18}O$ values also shows a positive excursion, from -8‰ to about -3‰, but returning to almost -8‰ at the top of the section (Fig. 4).

Strontium isotopes

Based on the Rb and Sr contents, 10 samples were selected for Sr isotopic analysis (Table 3).

According to Halverson *et al.* (2007), the Sr concentration ([Sr]) itself is the most efficient parameter to monitor the potential preservation of primary $^{87}Sr/^{86}Sr$ signatures, because diagenetic alteration result in a sharp increase in the $^{87}Sr/^{86}Sr$ ratio beyond a threshold [Sr], as predicted by water-rock interaction models (*e.g.* Jacobsen & Kaufman 1999). Since the initial rock [Sr] can differ substantially based on the mineralogy (*e.g.* calcite vs. aragonite) and on the seawater [Sr], this threshold is specific for each rock, and can be seen on a $^{87}Sr/^{86}Sr$ *vs.* [Sr] diagram.

Based on this procedure, a threshold of 750 ppm Sr was established for the Arcos carbonates, below which the ratios were considered altered. Thus, only four samples — M40 (1618 ppm), M45 (1817 ppm), M46 (1957 ppm) and M48 (3303 ppm) — had their isotopic signature considered as primary, all located in the uppermost portion of the section. These samples yielded $^{87}Sr/^{86}Sr$ ratios, varying from 0.7075 to 0.7077.

DISCUSSION

General features

The major and trace elements patterns were strongly controlled by the terrigenous content in the carbonate rocks,

as indicated by the high concentrations in Si, K, Al, Ti and other litophile elements observed in the samples from the Units 2 and 3. In Unit 2, the terrigenous phases occur in sand and silt size, while in Unit 3 they are clay-sized. As REE concentrate mainly in the finer fractions (McLennan 1989), Unit 3 shows higher REE content than Unit 2.

The geochemical signature of Unit 4 is coherent with its muddy composition, but shows high K relative to Na

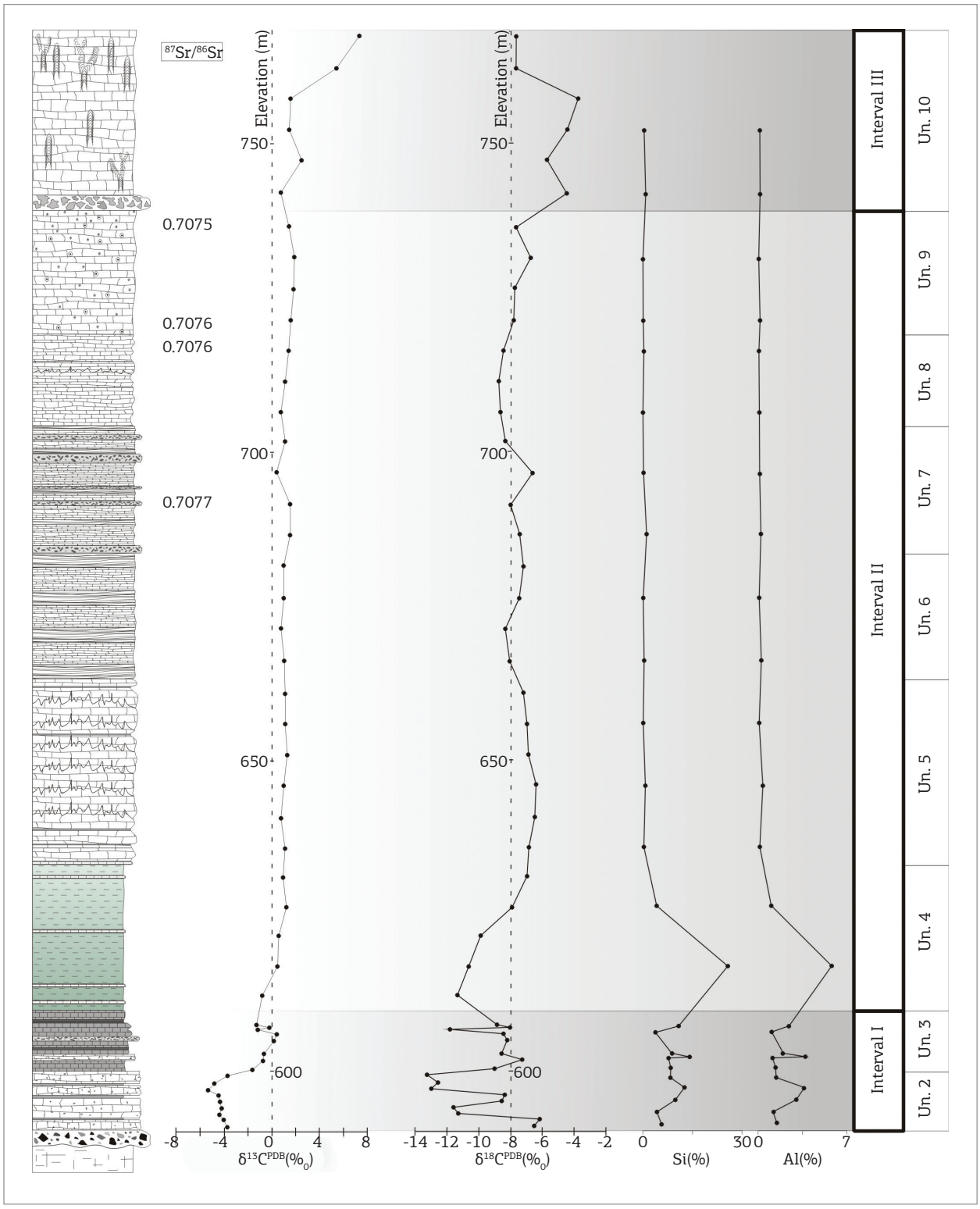

Figure 4. Chemostratigraphic variation of $\delta^{13}C_{PDB}$, $\delta^{18}O_{PDB}$ and $^{87}Sr/^{86}Sr$ in the studied section.

Table 3. $\delta^{13}C$, $\delta^{18}O$ and Sr isotopic data from Sete Lagoas Formation at Arcos, Minas Gerais.

Sample	$\delta^{13}C$	$\delta^{18}O$	Rb (ppm)	Sr (ppm)	$^{87}Sr/^{86}Sr$ ($\pm 2\sigma$)
M3	-3.72	-6.49	_	_	_
M4	-4.05	-6.18	_	_	_
M5	-4.38	-11.27	_	_	_
M6	-4.23	-11.59	_	_	_
M7	-4.37	-8.56	_	_	_
M8	-4.44	-8.37	_	_	_
M9	-5.38	-12.99	_	_	_
M10	-4.83	-12.57	_	_	_
M12	-3.73	-13.24	_	_	_
M13	-1.64	-8.99	_	_	_
M15	-0.73	-7.26	_	_	_
M17	-0.71	-8.54	_	_	_
M18	0.15	-8.21	11	174	0.715348 (48)
M19	0.39	-8.44	_	_	_
M20	-1.14	-11.81	14	292	0.709992 (8)
M21	-0.19	-8.06	_	_	_
M22	-1.27	-8.84	_	_	_
M24	-0.80	-11.36	_	_	_
M25	0.43	-10.65	_	_	_
M26	0.56	-9.89	_	_	_
M27	1.24	-7.90	_	_	_
M28	0.93	-6.95	_	_	_
M29	1.08	-6.84	7	304	0.708271 (42)
M30	0.75	-6.47	_	_	_
M31	0.98	-6.40	_	_	_
M32	1.27	-6.87	_	_	_
M33	1.12	-6.97	_	_	_
M34	1.10	-7.18	_	_	_
M35	1.05	-8.06	_	_	_
M36	0.77	-8.34	5	401	0.708057 (20)
M37	1.00	-7.44	3	414	0.707804 (22)
M38	0.98	-7.18	_	_	_
M39	1.50	-7.40	_	_	_
M40	1.52	-7.99	3	1618	0.707683 (72)
M41	0.40	-6.63	_	_	_
M42	1.11	-8.32	_	_	_

Continue...

Table 3. Continuation.

Sample	$\delta^{13}C$	$\delta^{18}O$	Rb (ppm)	Sr (ppm)	$^{87}Sr/^{86}Sr$ ($\pm 2\sigma$)
M43	0.73	-8.61	_	_	_
M44	1.14	-8.73	_	_	_
M45	1.43	-8.43	1	1817	0.707622 (40)
M46	1.61	-7.80	1	1957	0.707648 (23)
M47	1.83	-7.73	_	_	_
M48	1.91	-6.74	0	3303	0.707493 (20)
M49	1.43	-7.66	_	_	_
M50	0.77	-4.47	_	_	_
M51	2.50	-5.70	_	_	_
M52	1.49	-4.42	_	_	_
M53	1.61	-3.73	_	_	_
M54	5.41	-7.64	_	_	_
M55	7.34	-7.63	25	678	0.708009 (22)

*$\delta^{13}C$ and $\delta^{18}O$ values in ‰ PDB (normalized to Pee Dee Belemnite)

and a strong depletion in Cu and Pb relative to the standard shale. This pattern may reflect the source rock of the sediments and, in the case of the alkalis, should be related to the clay mineral type. In this case, one possibility is the predominance of illite group clay minerals.

Diagenetic alteration

The evaluation of the element behavior, integrated with the isotopic data, allows the identification and characterization of the processes which affected the rock after its deposition. The $\delta^{18}O$ values are commonly used for this purpose since they hardly preserve the primary isotopic composition of seawater (Kaufman & Knoll 1995, Kah 2000).

The Mn/Sr ratio is used to detect diagenetic alteration by non-marine fluids. All the analyzed samples show Mn/Sr ratios below 10 (from 0.02 to 7.87), which is the limit defined by Kaufman and Knoll (1995) for unaltered samples. However, ratios higher than 0.8 only occur in samples from Units 2 and 3, possibly due to their higher terrigenous content (Tab. 1). In the purely carbonate units, the values are always below 0.8, attending the more rigorous limit proposed by Veizer *et al.* (1983). These data indicate that the analyzed rocks were not significantly altered by non marine diagenetic fluids, ensuring the primary nature of the carbon isotopic signal.

High Mn levels in the carbonates can indicate interaction with Mn-rich fluids (Jacobsen & Kaufman 1999), or even represent a primary feature, related to the seawater composition (Halverson *et al.* 2004, Font *et al.* 2006). Among the studied rocks, the calcitic dolomites of Unit 3 present the highest Mn contents and the lowest Sr/Ca ratios, suggesting that the dolomitization process was influenced by Sr-poor, Mn rich fluids. Additionally, the high Mn levels may be a genetic feature, as proposed by Font *et al.* (2006) for other cap carbonates. The low Sr content, in this case, could also have been caused by Sr loss during dolomitization, as seen in many other carbonate sequences (James & Jones 2015, Bartley *et al.* 2007). It is not discarded, however, that this signature has been affected by the high terrigenous content of Unit 3.

According to Kah (2000), during the diagenetic process, a decrease in $\delta^{18}O$ values with respective increase in the Mn may occur if the carbonates interact with isotopically light fluids, such as freshwater. In the case of interaction with isotopically heavy fluids (*e.g.* evaporitic brines, interstitial rising water), there would have an increase in the $\delta^{18}O$ values. In the Arcos carbonates, the samples do not follow any of the two directions, suggesting that diagenetic processes were not influenced by these fluids.

Depositional conditions

In the analyzed section, there is no strict relationship between the sedimentary facies and the REE+Y pattern. Y/Ho ratios of the Bambuí carbonates (Tab. 2) show an average value of 35.7, clearly lower than the seawater standard (c. 60-90). Considering that reference values for fluvial water are above those of PAAS (c. 27) and below the seawater, the obtained ratios may indicate an expressive mixing of fresh

water during the carbonate deposition. This hypothesis is endorsed by the high $^{87}Sr/^{86}Sr$ ratios (Tab. 3), which may result of fresh water addition during carbonate sedimentation (Zhao *et al*. 2009).

In the light of the regional geological context, a possible mixing of freshwater with seawater during the carbonate deposition could be explained by the melting of the ice sheets which could have covered the whole region. Additionally, deglaciation process should cause dramatic climatic changes (Hoffman & Schrag 2002, Allen & Hoffman 2005), resulting in an input of isotopically light meltwater into the ocean.

Carbon and Oxygen isotopes

The studied C isotopic section shows a similar pattern of other Neoproterozoic carbonate successions in Brazil and in several Gondwana sucessions, allowing considerations about the prevailing environment at the time of deposition.

The strong negative $\delta^{13}C$ excursion in the Interval I may be interpreted as a period of intense decrease in the biological activity. To the top of the section, the increase of the $\delta^{13}C$ values would indicate a progressive increase of biological activity and the restoration of atmosphere/sea interaction.

The Interval I isotopic signatures, together with the sedimentary conditions of Unit 1, and the occurrence of aragonite fans in Unit 3 allow to interpret the Units 2 and 3 as cap carbonates, deposited in a post-glacial environment. Similar features have been used to identify cap carbonates worldwide (*e.g.* Kaufman *et al.* 1991, Hoffman *et al*. 1998, Santos *et al.* 2000, 2004, Font *et al.* 2006, Alvarenga *et al.* 2008) and also in other parts of the São Francisco Basin (Vieira *et al.* 2007).

The relatively constant $\delta^{13}C$ values in the Interval II may indicate a period of stable bioproductivity reflecting also stable environmental conditions (light, temperature, etc.). The sharp increase in $\delta^{13}C$ values during Interval III suggests a quick rise in bioproductivity, endorsed by the profusion of stromatolitic constructions that occur in the Unit 10. Positive excursions of $\delta^{13}C$ values were reported in some Neoproterozoic carbonate sequences in South America, Africa, Greenland, North America and Asia (Santos *et al*. 2000, 2004, Misi *at al*. 2007 and references therein) and also in other parts of the São Francisco Basin. Also, the general isotopic pattern recognized in Arcos carbonates has correlatives in several post-glacial carbonate sequences worldwide (*e.g.* Otavi Group, Namibia).

Oxygen isotopes are not usually considered in paleoenvironmental studies because the Precambrian carbonates hardly ever record the seawater oxygen isotopic composition (Kah 2000). In fact, the $\delta^{18}O$ values determined on our samples cover almost the whole spectrum of the global variation curve proposed by Jacobsen and Kaufman (1999), preventing a reliable correlation. In addition, no correlation between $\delta^{18}O$ and the different sedimentation environments is observed in the studied section.

Strontium isotopes

The $^{87}Sr/^{86}Sr$ ratios obtained in Arcos carbonates are between 0.7075 and 0.7077, which contrast with the available Sr global evolution curves (e.g. Halverson *et al.* 2007) for the end of the Ediacaran, when ratios as high as 0.7080 are expected. The same discrepancy was noted by Paula-Santos *et al.* (2015) in other studied sections of the Bambuí Basin, and also occurs in other Ediacaran basins around the world (e.g. Gaucher *et al.* 2004, Gómez Peral *et al.* 2007, Boggiani *et al.* 2010, Frei *et al*. 2011).

Such discrepancies points to the prevalence of local controls in marine Sr composition, rather than global processes. Concerning the Bambuí Basin, it could indicate the influence of freshwater mixing and/or the restricted conditions of the basin, which could prevent or hamper the homogenization with the global ocean (Paula-Santos *et al.* 2015).

We consider that, due to such situations, blind dating based on isotope chemostratigraphy should be avoided, and interbasinal correlations should proceed carefully, especially in the case of potentially restricted basins.

Positive excursion of $\delta^{13}C$

The remarkable positive excursion of $\delta^{13}C$ values in the Interval III is an important anomaly, which is also described in other parts of the basin (Iyer *et al*. 1995, Santos *et al*. 2000, 2004, Vieira *et al*. 2007). Its large geographic distribution suggests an alteration of the C reservoir in regional or even global scale (Santos *et al.* 2000).

The obtained $\delta^{13}C$ curve may be compared with other data from the São Francisco Basin based on the positive excursion (Fig. 5). The similarity with the "Bocaina Quarry" curve, also obtained in the western portion of the basin, is notable, where the positive excursion occurs at the top of more than one hundred meters. In some other sections the isotopic shift is observed a few tens of meters from the bottom of the unit. These significant differences reflect the heterogeneity of the basin's filling, possibly related to their paleogeography.

In the studied sequence, the $\delta^{13}C$ isotopic shift coincides with the appearance of common stromatolitic bodies and marks the beginning of dolomite predominance (Unit 10). The coincidence of this anomaly and the continuous layer of collapse breccias suggests that these rocks should record an important event at basin scale.

Several hypotheses have been suggested to explain the expressive positive $\delta^{13}C$ excursions. Besides a dramatic increase of bioproductivity, such features could

have been caused by alterations in the balance between inorganic and organic C reservoir, due to changes in the burial rates of organic matter (Knoll *et al.* 1986, Iyer *et al.* 1995). Other possibilities may be the deposition in evaporitic environment (Mees *et al.* 1998), the reduction of CO_2 and sulphides, and changes in the basin paleogeography possibly caused by tectonics (Santos *et al*. 2000).

As previously considered by Santos *et al.* (2000), the tectonics may have played an important role in the genesis of this C anomaly, creating paleogeographic conditions favorable to the biological development (*e.g* vast shallow platforms). Such assertive seems reasonable if considered that, at the time of deposition of these rocks, the tectonic stress responsible for the rise of the Brasília Belt and, possibly, of the Araçuaí Orogen, were already active (Kuchenbecker 2011, 2014, Martins-Neto & Alkmim 2001, Martins-Neto 2009, Reis 2011).

It may be also considered that the positive $\delta^{13}C$ excursion is followed by a rise in the $\delta^{18}O$ values. This data could suggest that the anomaly could be related to confined conditions of the basin, implying in rising of evaporation rate and changes in the biological conditions. This scenario seems to be possible due to the basin geotectonic framework: in this case, the anomaly could record the moment when the basin was completely isolated from the global ocean by the tectonic activity in the surrounding orogenic belts, creating a restricted marine environment.

Inter and intrabasinal correlations

Our isotopic data are compatible with other C-O profiles reported for the Sete Lagoas Formation in other parts of the Bambuí Basin.

Alvarenga *et al.* (2007) report $\delta^{13}C$ values of about -6‰ in cap dolostones in the Bezerra area (Goiás State), which to the top turn to high positive values, close to 9‰. The $^{87}Sr/^{86}Sr$ reported for that section is close to 0.7075, quite similar to the ratios presented here. Similar $\delta^{13}C$ profiles are described by Vieira *et al.* (2007) in carbonates from Sete Lagoas Formation, next to Sete Lagoas city (Minas Gerais State), and by Santos *et al.* (2000) in carbonates of the same unit near São Domingos range (Minas Gerais) and São Domingos city (Goiás state). In all cases, the lower Sete Lagoas Formation was interpreted as cap carbonates.

In terms of interbasinal features, $\delta^{13}C$ patterns quite similar to those found in Arcos were described in other sucessions worldwide. Among those that show more remarkable similarities, highlights for the Frecheirinha Formation (northeastern Ceará State, Brazil, Sial *et al.* 2000), the Olhos D'Água Formation (Sergipano Belt, Brazil, Sial *et al.* 2010), the upper Otavi Group (Namibia, Kaufman et al. 2009) and the carbonates from Bloeddrif Member, in Gariep Belt (Namibia, Frimmel 2009), which shows remarkable correlations also in the REE patterns.

Glaciation age

The obtained data indicate that in the Arcos region the Carrancas and Sete Lagoas formations represent a "tillite-cap

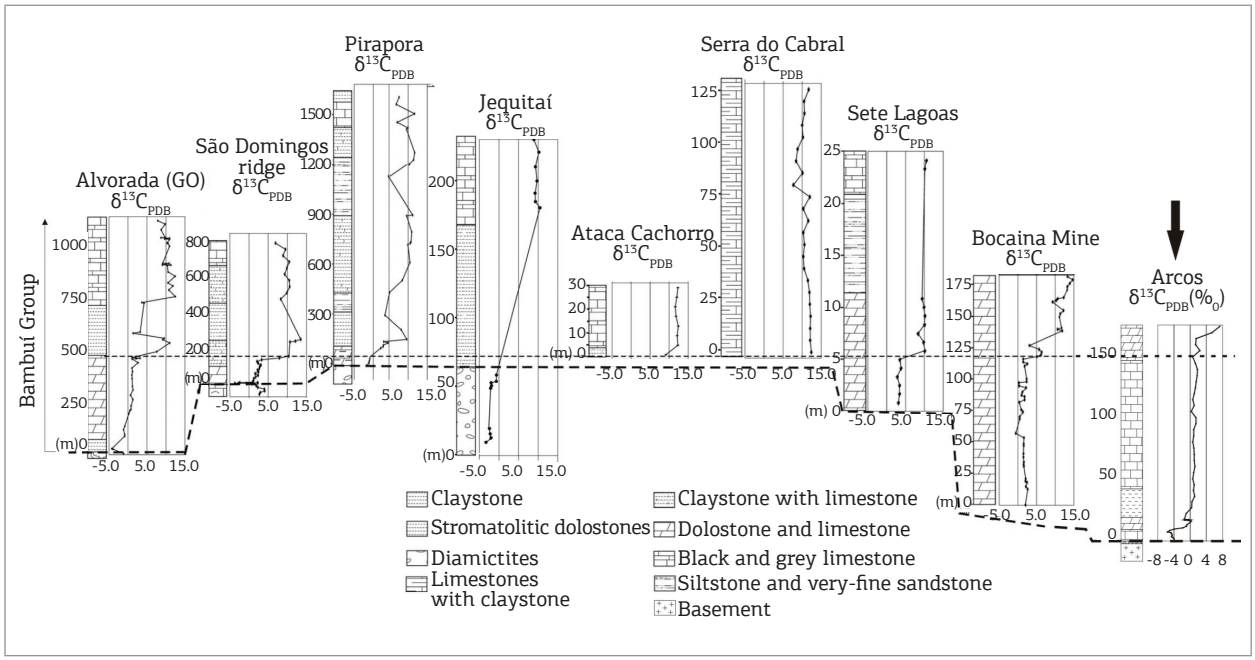

Figure 5. Comparison of some isotopic profiles of the São Francisco Basin, with the positive $\delta^{13}C_{PDB}$ excursion as datum. Arrow indicates the section studied in this work. Modified from Santos *et al.* (2004).

carbonate" pair, as usually found in several Neoproterozoic deposits worldwide. However, a question still remains: to which glaciation does it belong?

The Sete Lagoas Formation was previously interpreted as a record of the Sturtian (Vieira *et al.* 2007, Babinski *et al.* 2007) or Marinoan (Kuchenbecker 2011, Caxito *et al.* 2012) glaciations. The new geochronological and paleontological data, however, indicates that the unit is not related to these glaciations, but could record a younger one (Paula-Santos *et al.* 2015). In this sense, Kuchenbecker (2014) considered a possible correlation with the glacial events between 548 and 542 Ma, which are recorded in the Nama Basin, southwest Africa, with possible equivalents in the West Congo Group (Germs 1995, Frimmel *et al.* 2006; Germs & Gaucher, 2012).

Contrary to what occurs with the Carrancas Formation, the relationship between the Jequitaí Formation and the Bambuí Group is not well established. Only at the Bicudo Ridge the Sete Lagoas limestones lies on the Jequitaí diamictites, and even there the true contact is not visible (Prezotti *et al.* 2010). Thus, it is possible that the Jequitaí Formation records the Sturtian event (as well as the Macaúbas Group) and has not relationship with the Bambuí Group. The same conclusion was drawn by Reis and Suss (2014), by using drill core data and seismic information. It is also possible that the carbonates from Sambra quarry, dated at 740 Ma by Babinski *et al.* (2007), represent the cap carbonate of such event, as proposed by Alkmim and Martins-Neto (2012).

CONCLUSIONS

The Bambuí Group at Arcos region (Minas Gerais) is represented by a tillite layer assigned to the Carrancas Formation, and by a thick carbonate sequence with mudstone layers, assigned to the Sete Lagoas Formations. The stratigraphic data show progradational-retrogradational-progradational cycles that record, above the glacial sediments, shelf environments ranging from coastal, wave-influenced, to deeper ones, dominated by mud deposition.

The basal carbonate rocks are very impure and the terrigenous content controls the lithochemical signature. The rest of the carbonates are pure, and its geochemical patterns do not show signals of post depositional alteration, and reflect the seawater composition. Y/Ho ratios ranging from 25 to 50 suggest a freshwater input during carbonate deposition and this process could be responsible for the discrepancy of $^{86}Sr/^{87}Sr$ ratios in relation to the Sr global evolution curves.

Such a discrepancy, coupled with the indication of fresh water contribution during sedimentation and the possibility of a restricted marine environment, leads us to discuss the applicability of the overall variation curves.

Based on the $\delta^{13}C$ profile and petrological features (especially the aragonite fans), it is concluded that the basal units (Units 2 and 3) of the Sete Lagoas Formation represent a cap carbonate. The geotectonic framework of the western São Francisco Basin suggests a correlation with the glacial events between 548 and 542 Ma, which are recorded in the Nama Basin, southwest Africa.

The remarkable positive $\delta^{13}C$ excursion seen at the top of the studied section represents a regional anomaly, reported also in other portions of the basin (*e.g.* Iyer *et al.* 1995, Santos *et al.* 2000, 2004, Vieira *et al.* 2007). Due to the regional geotectonic setting during the Neoproterozoic, it is considered that this anomaly could have had a tectonic driver.

In summary, the available dataset from the Bambuí Basin allow us to envisage, by the very end of the Neoproterozoic, a restricted marine basin surrounded by mountain belts in the inner Gondwana. In its early stages, the sedimentation was influenced by a glacial episode, whose end was responsible to a substantial freshwater input in the basin. The gradual temperature rise was followed by the progressive increase in marine biologic activity. To the top, a sudden rise in bioproductivity could also have been driven by tectonic related paleogeographic changes.

ACKNOWLEDGEMENTS

The authors acknowledge financial support provided by CODEMIG (Companhia de Desenvolvimento Econômico do Estado de Minas Gerais), CNPq (Conselho Nacional de Desenvolvimento Científico e Tecnológico), and FAPESP (Fundação de Apoio à Pesquisa do Estado de São Paulo). We also thank R.D. Costa, D.G.C. Fragoso, H.L.S. Reis, R.V. Santos, A. Uhlein, as well as L. Gómez-Peral and an anonymous reviewer for comments and suggestions.

REFERENCES

Alkmim F.F. & Martins-Neto M. A. 2012. Proterozoic first-order sedimentary sequences of the São Francisco craton, eastern Brazil. *Marine and Petroleum Geology,* **33**(1):127-139.

Allen P.A. & Hoffmann P. F. 2005. Extreme winds and waves in the aftermath of a Neoproterozoic glaciation. *Nature,* **433**:123-127.

Alvarenga C.J.S., Della Giustina M.E.S., Silva N.G.C., Santos R.V.S., Gioia S.M.C.L., Guimarães E.M., Dardenne M.A., Sial A.N., Ferreira V.P. 2007. Variações dos isótopos de C e Sr em carbonatos pré e pós-glaciação Jequitaí (Esturtiano) na região de Bezerra-Formosa, Goiás. *Revista Brasileira de Geociências,* **37**(4):147-155.

Alvarenga C.J.S., Dardenne M.A., Santos R.V., Brod E.R., Gioia S.M.C.L., Sial A.N., Dantas E.L., Ferreira V.P., 2008. Isotope stratigraphy of Neoproterozoic cap carbonates in the Araras Group, Brazil. *Gondwana Research*, **13**:469-479.

Alvarenga C.J.S., Dardenne M.A., Vieira L.C., Martinho C.T., Guimarães E.M., Santos R.V., Santana R.O. 2012. Estratigrafia da borda ocidental da Bacia do São Francisco. *Boletim de Geociências da PETROBRAS* (Impresso), **20**:145-164.

Babinski M., Vieira L.C., Trindade R.I.F. 2007. Direct dating of the Sete Lagoas cap carbonate (Bambuí Group, Brazil) and implications for the Neoproterozoic glacial events. *Terra Nova*, **19**:401-406.

Bartley,J.K., Kah L.C., McWilliams J.L., Stagner A.F. 2007. Carbon isotope chemostratigraphy of the Middle Riphean type section (Avzyan Formation, Southern Urals, Russia): Signal recovery in a fold-and-thrust belt. *Chemical Geology,* **237**:211-232.

Boggiani P.C., Gaucher C., Sial A.N., Babinski M., Simon C.M., Riccomini C., Ferreira V.P., Fairchild T.R., 2010. Chemostratigraphy of the Tamengo Formation (Corumbá Group, Brazil): a contribution to the calibration of the Ediacaran carbon-isotope curve. Precambrian *Research*, **182**(4):382-401.

Caxito F.de A., Halverson G. P., Uhlein A., Stevenson R., Gonçalves-Dias T., Uhlein G.J. 2012. Marinoan glaciation in east central Brazil. *Precambrian Research,* **200-203**:38-58.

Coelho J.C.C., Martins-Neto M.A., Marinho M.S. 2008. Estilos estruturais e evolução tectônica da porção mineira da bacia proterozóica do São Francisco. *Revista Brasileira de Geociências*, **38**(2):149-165.

Delpomdor F. & Préat A. 2013. Early and late Neoproterozoic C, O and Sr isotope chemostratigraphy in the carbonates ofWest Congo and Mbuji-Mayi supergroups: A preserved marine signature? *Palaeogeography, Palaeoclimatology, Palaeoecology,* **389**:35-47.

Fernandes R.A. & Carneiro M.A. 2000. O Complexo Metamórfico Campo Belo (Cráton São Francisco Meridional): unidades litodêmicas e evolução tectônica. *Revista Brasileira Geociências*, **30**:671-678.

Figueiredo M.F. 2006. *Quimioestratigrafia das rochas ediacarianas do extremo norte da Faixa Parguai, Mato Grosso.* Master's Dissertation, Geosciences Institute, Universidade de São Paulo, Brazil. 119 p.

Figueiredo M.F. 2010. *Quimioestratigrafia isotópica (C, O, S e Sr), geocronologia (Pb-Pb e K-Ar) e proveniência (Sm-Nd) das rochas da Faixa Paraguai Norte, Mato Grosso.* PhD Thesis, Geosciences Institute, Universidade de São Paulo, Brazil. 198 p.

Font E., Nédélec A., Trindade R.I.F., Macouin M., Charrière A. 2006. Chemostratigraphy of the Neoproterozoic Mirassol d'Oeste cap dolostones (Mato Grosso, Brazil): An alternative model for Marinoan cap dolostone formation. *Earth and Planetary Science Letters,* **250**:89-103.

Frei R., Gaucher C., Døssing L.N., Sial A.N. 2011. Chromium isotopes in carbonates – a tracer for climate change and for reconstructing the redox state of ancient seawater. *Earth and Planetary Science Letters*, **312**:114-125.

Frimmel H.E., Tack L. Basei M.S., Nutman A.P., Boven A. 2006. Provenance and chemostratigraphy of the Neoproterozoic West Congolian Group in the Democratic Republic of Congo. *Journal of African Earth Sciences,* **46**:221-239.

Frimmel H.E. 2008. *REE geochemistry of Neoproterozoic carbonates: Deviations from normal marine signatures.* International Geological Congress, Oslo. MPC-03, p. 1, D-Rom.

Frimmel H.E., 2009. Trace element distribution in Neoproterozoic carbonates as palaeoenvironmental indicator. *Chemical Geology,* **258**:338-353.

Gaucher C., Sial A.N., Blanco G., Sprechmann P. 2004. Chemostratigraphy of the Lower Arroyo del Soldado Group (Vendian, Uruguay) and Paleoclimatic Implications. *Gondwana Research*, **7**(3):715-730.

Gaucher C. & Germs G.J.B. 2009. Skeletonised metazoans and protists. Neoproterozoic–Cambrian biota. *In*: Gaucher C., Sial A.N., Halverson G.P., Frimmel H.E. (Eds.). Neoproterozoic-Cambrian Tectonics, Global Change and Evolution: A Focus on Southwestern Gondwana. *Developments in Precambrian Geology*, v. 16. Elsevier, pp. 327–338.

Germs G.J.B. 1995. The Neoproterozoic of southwestern Africa, with emphasis on platform stratigraphy and paleontology. *Precambrian Research,* **73**:137-151.

Gómez Peral L.E., Poiré D.G., Strauss H., Zimmermann U. 2007. Chemostratigraphy and diagenetic constraints on Neoproterozoic carbonate successions from the Sierras Bayas Group, Tandilia System, Argentina. *Chemical Geology,* **237**:109-128.

Halverson G.P., Maloof A., Hoffman P. 2004. The Marinoan Glaciation (Neoproterozoic) in northeast Svalbard. *Basin Research,* **16**:297-324.

Halverson G.P., Hoffman P.F., Schrag D.P., Maloof A.C. 2005. Toward a Neoproterozoic composite carbon-isotope record. *Geological Society of America,* **117**(9):1181-1207.

Halverson G.P., Dudás F.O., Maloof A.C., Bowring S.A. 2007. Evolution of the $^{87}Sr/^{86}Sr$ composition of Neoproterozoic seawater. *Palaeogeography, Palaeoclimatology, Palaeoecology,* **256**:103-129.

Halverson G.P., Wade B.P., Hurtgen M.T., Barovich K.M. 2010. Neoproterozoic chemostratigraphy. *Precambrian Research,* **182**:337-350.

Hoffman P.F., Kaufman A.J., Halverson G.P., Schrag D.P. 1998. A Neoproterozoic Snowball *Earth. Science,* **281**:1342-1346.

Hoffman P.F. & Schrag D.P. 2002. The Snowball Earth hypothesis: testing the limits of global change. *Terra Nova,* **14**(3):129-155.

Iyer S.S., Babinski M., Krouse H.R., Chemale Jr. F. 1995. Highly ^{13}C enriched carbonate and organic matter in the Neoproterozoic sediments of the Bambuí Group, Brazil. *Precambrian Research,* **73**:271-282.

Jacobsen S. & Kaufman A. 1999. The Sr, C and O isotopic evolution of the Neoproterozoic seawater. *Chemical Geology,* **161**:37-57.

James N.P. & Jones B. 2015. *Origin of carbonate sedimentary rocks.* John Willey and Sons, 464 p.

Kah L.C. 2000. Depositional $\delta^{18}O$ signatures in Proterozoic dolostones: constraints on seawater chemistry and early diagenesis. *In*: Grotzinger J.P. & James N.P. (eds.). *Carbonate sedimentation and diagenesis in the involving Precambrian World*. Society for Sedimentary Geology, Special Publication 67.

Kaufman A.J. & Knoll A.H. 1995. Neoproterozoic variations in the C-isotopic composicional of seawater: Stratigraphic and biogeochemical implications. *Precambrian Research,* **73**:27-49.

Kaufman A.J., Hayes J.M., Knoll A.H., Germs G.J.B. 1991. Isotopic composition of carbonates and organic carbon from upper Proterozoic successions in Namibia: Stratigraphic variation and the effects of diagenesis and metamorphism. *Precambrian Research,* **49**:301-327.

Kaufman A.J., Sial A.N., Frimmel H.E., Misi A. 2009. Neoproterozoic to Cambrian palaeoclimatic events in southwestern Gondwana. *In*: Gaucher C., Sial A.N., Halverson G.P., Frimmel H.E. (Eds.). *Neoproterozoic-Cambrian Tectonics, Global Change and Evolution: A Focus on Southwestern Gondwana*. Developments in Precambrian Geology, v. 16. Elsevier, pp. 369-388.

Knoll A.H., Hayes J.M., Kaufman A.J., Swett K., Lambert I.B. 1986. Secular variation in carbon isotope ratios from upper Proterozoic successions of Svalbard and East Greenland. *Nature,* **321**:832-837.

Kuchenbecker M. 2011. *Quimioestratigrafia e proveniência sedimentar da porção basal do Grupo Bambuí em Arcos (MG)*. Master's Thesis, Universidade Federal de Minas Gerais, Belo Horizonte, 91 p.

Kuchenbecker M. 2014. Relações entre coberturas do Cráton do São Francisco e bacias situadas em orógenos marginais: o registro de datações U-Pb de grãos detríticos de zircão e suas implicações geotectônicas. PhD Thesis. Universidade Federal de Minas Gerais.

Kuchenbecker M., Babinski M., Pedrosa-Soares A.C., Lopes-Silva L., Pimenta F., Rossi M.G., Dias P.H.A. 2010. Isotopic approach of the basement/cover boundary in Arcos region (Brazil): New evidence of a Neoproterozoic glaciation in the São Francisco basin. *In*: South American Symposium on Isotopic Geology 7, Brasília, Brazil. *Short Papers*, 305-308.

Kuchenbecker M., Lopes-Silva L.L., Pimenta F., Pedrosa-Soares A.C., Babinski M. 2011. Estratigrafia da porção basal do Grupo Bambuí na região de Arcos (MG): uma contribuição com base em testemunhos de sondagem. *Geologia USP – Série Científica*, **11**(2):45-54.

Kuchenbecker M., Babinski M., Pedrosa-Soares A.C., Costa R.D., Lopes-Silva L., Pimenta F. 2013. Provenance and sedimentary analysis of the basal portion of the Bambuí Group at Arcos (MG). *Geologia USP – Série Científica*, **13**(4):4-61. Martins-Neto M.A. 2009. Sequence stratigraphic framework of Proterozoic successions in eastern Brazil. *Marine and Petroleum Geology,* **26**:163-176.

Martins-Neto M.A., Alkmim F.F. 2001. Estratigrafia e evolução tectônica das bacias neoproterozóicas do paleocontinente São Francisco e suas margens: Registro da quebra de Rodínia e colagem de Gondwana. *In:* Pinto C.P. , Martins-Neto M.A. (eds.) *Bacia do São Francisco: Geologia e Recursos Naturais*, SBG/Núcleo MG, pp. 31-54.

Martins-Neto M.A., Pedrosa-Soares A.C., Lima S.A.A. 2001. Tectono-sedimentary evolution of sedimentary basins from Late Paleoproterozoic to Late Neoproterozoic in the São Francisco craton and Araçuaí fold belt, eastern Brazil. *Sedimentary Geology,* **141/142**:343-370.

McLennan S.M. 1989. Rare earth elements in sedimentary rocks: Influence of provenance and sedimentary processes. *Reviews in Mineralogy,* **21**:169-200.

Mees F., Reyes E., Keppens E. 1998. Stable isotope geochemistry of gaylussite and nacholite from the deposits of the crater Lake at Malha, northern Sudan. *Chemical Geology,* **146**:87-98.

Melezhik V., Gorokhov I., Kuznetsov A., Fallick A., 2001. Chemostratigraphy of Neoproterozoic carbonates: implications for 'blind dating'. *Terra Nova,* **13**:1–11.

Misi A., Kaufman A.J., Veizer J., Powis K., Azmy K., Boggiani P.C., Gaucher C.,Teixeira J.B.G., Sanches A.L., Iyer S.S. 2007. Chemostratigraphic correlation of Neoproterozoic successions in South America. *Chemical Geology*, **237**:22-45.

Noce C.M., Teixeira W., Quéméneuer J.J.G., Martins V.T.S., Bolzachini E. 2000. Isotopic signatures of Paleoproterozoic granitoids from the southern São Francisco Craton and implications for the evolution of the Transamazonian Orogeny. *Journal of South American Earth Sciences*, **13**:225-239.

Noce C.M., Pedrosa-Soares A.C., Silva L.C., Alkmim F.F. 2007. O embasamento arqueano e paleoproterozóico do Orógeno Araçuaí. *Geonomos*, **15**(1):17-23.

Oliveira A.H. & Carneiro M.A. 2001. Campo Belo Metamorphic Complex: Tectonic evolution of an Archean sialic crust of the southern São Francisco Craton in Minas Gerais (Brazil). *Anais da Academia Brasileira de Ciências,* **73**(3):397-415.

Paula-Santos G.M., Babinski M., Kuchenbecker M., Caetano-Filho S., Trindade R.I.F., Pedrosa-Soares A.C. 2015. New evidence of an Ediacaran age for the Bambuí Group in southern São Francisco craton (eastern Brazil) from zircon U-Pb data and isotope chemostratigraphy. *Gondwana Research*, **28**:702-720.

Pimentel M., Rodrigues J.B., DellaGiustina M.E.S., Matteini S.J.M., Armstrong R. 2011. The tectonic evolution of the Neoproterozoic Brasília Belt, central Brazil, based on SHRIMP and LA-ICPMS U-Pb sedimentary provenance data: A review. *Journal of South American Earth Sciences,* **31**:345-357.

Pimentel M., Della Giustina M.E.S., Rodrigues J.B., Junges S.L. 2012. Idades dos grupos Araxá e Bambuí: Implicações para a evolução da Faixa Brasília. *In*: Brazilian Geological Congress 46, Santos. *Resumos*, CD-ROM.

Prezotti F., Murta H., Tedeschi M. 2010. *Mapeamento Geológico da Porção Sul da Serra do Bicudo, Corinto-MG*. Graduation dissertation, Universidade Federal de Minas Gerais, Belo Horizonte, 71 p.

Reis H.L.S. 2011. *Estratigrafia e tectônica da Bacia do São Francisco na zona de emanações de gás natural do baixo Rio Indaiá (MG)*. Master's Thesis. Universidade Federal de Ouro Preto, Ouro Preto, 126 p.

Reis H.L.S. & Suss J. Os depósitos glaciogênicos da Bacia do São Francisco (MG): registro de um ou dois episódios glaciais? *In*: *Anais do 47º Congresso Brasileiro de Geologia*, Salvador. SBG.

Rodrigues J.B. 2008. *Proveniência de sedimentos dos grupos Canastra, Ibiá, Vazante e Bambuí – Um estudo de zircões detríticos e Idades Modelo Sm-Nd*. PhD Thesis, Instituto de Geociências, Universidade de Brasília, Brazil.

Romano A.W. & Knauer L.G. 2003. Evidências da glaciação neoproterozoica na base do Grupo Bambuí - região de Onça do Pitangui - Minas Gerais. *In*: Simpósio de Gelogia de Minas Gerais, 12, *Anais*, v. 1

Santos R.V., Alvarenga C.J.S., Dardenne M.A., Sial A.N., Ferreira V.P. 2000. Carbon and oxygen isotope profiles across Meso-Neoproterozoic limestones from central Brazil: Bambuí and Paranoá groups. *Precambrian Research,* **104**:107-122.

Santos R.V., Alvarenga C.J.S., Babinski M., Ramos M.L.S, Cukrov N., Fonseca M.A., Sial A.N., Dardenne M.A., Noce C.M. 2004. Carbon isotopes of Mesoproterozoic-Neoproterozoic sequences from Southern sao Francisco craton and Araçuaí Belt, Brazil: Paleogeographic implications. *Journal of South American Earth Sciences*, **18**:27-39.

Shields G. & Veizer J. 2002. Precambrian marine carbonate isotope database: Version 1.1. *Geochemistry, Geophysics, Geosystems*, **3**.

Sial A.N., Ferreira V.P., Almeida A.R., Romano A.W., Parente C., da Costa M.L., Santos V.H. 2000. Carbon isotope fluctuations in Precambrian carbonate sequences of several localities in Brazil. *Anais da Academia Brasileira de Ciências*, **72**:540-557.

Sial A.N., Gaucher C., Silva Filho M.A., Ferreira V.P., Pimentel M.M., Lacerda L.D., Emannoel V., Silva Filho E.V., Cezario W. 2010. C-Sr-isotope and Hg chemostratigraphy of Neoproterozoic cap carbonates of the Sergipano Belt, Northeastern Brazil. *Precambrian Research*, **182**:351-372.

Song C. Herong G., Linhua S., 2014. Geochemical characteristics of REE in the Late Neo-proterozoic limestone from northern Anhui Province, China. *Chinese Journal of Geochemistry*, **33**:187-193.

Veizer J., Compston W., Clauer N., Schidlowski, M., 1983. $^{87}Sr/^{86}Sr$ in Late Proterozoic carbonates: Evidence for a mantle event at 900 Ma ago. Geochimica et Cosmochimica Acta 47, 295-302.

Vieira L.C., Trindade R.I.F., Nogueira A.C.R., Ader M. 2007. Identification of a Sturtian cap carbonate in the Neoproterozoic Sete Lagoas carbonate platform, Bambuí Group, Brazil. *Comptes Rendus Geoscience*, **339**:240-258.

Warren L.V., Quaglio F., Riccomini C., Simões M.G., Poiré D.G., Strikis N.M., Anelli L.E., Strikis P.C. 2014. The puzzle assembled: Ediacaran guide fossil Cloudina reveals an old proto- Gondwana seaway. *Geology*, **42**(5):391-394.

Zhao Y., Zheng Y., Chen F. 2009. Trace element and strontium isotope constraints on sedimentary environment of Ediacaran carbonates in southern Anhui, South China. *Chemical Geology*, **265**:345-362.

Available at www.sbgeo.org.br